Published in final edited form as:
Dev Dyn. 2008 December ; 237(12): 3727–3737. doi:10.1002/dvdy.21781.

The effect of BMP signaling on development of the jaw skeleton

Diane Hu, **Celine Colnot**, and **Ralph S. Marcucio**[†]
Department of Orthopaedic Surgery, University of California at San Francisco, San Francisco, CA

Summary

Bone morphogenetic proteins (BMPs) regulate many aspects of development including skeletogenesis. Here, we examined the response of neural crest-derived cells to ectopic BMP signaling by infecting avian embryos with retroviruses encoding *Bmp-2* or *Bmp-4* at various times of development. Infection at stages 10 and 15 transformed large areas of the skull into cartilage by day 13. At this time cartilage condensations were still forming which revealed the presence of uncommitted mesenchymal cells. By day 19 hypertrophic chondrocytes were present in the cartilage possibly due to changes in the perichondrium that relieved repression on hypertrophy. While these cells expressed *Sox9*, *Collagen-2*, *Runx2*, *Ihh*, *Noggin*, and *Collagen-10*, cartilage was not replaced by bone. Whether this is an intrinsic property of the skull cartilage, or results from sustained Bmp signaling is not known.

Keywords

Bone morphogenetic protein; neural crest; cartilage; bone; muscle; *Runx2*; *Sox9*; *Fgf18*; *Twist-1*; craniofacial development; skeletal development

Introduction

Formation of the majority of the skeletal elements in the face use mechanisms that are distinct from the rest of the body. Throughout the appendicular and axial skeleton, bone forms primarily through endochondral ossification. During this process, chondrocytes form a cartilage template that is gradually removed by vascular invasion and subsequent osteogenesis. In contrast, in the face the formation of most of the cartilaginous and bony elements of the skeleton occurs independently of each other. The majority of cartilage that forms in the face remains as persistent cartilage that is not replaced by bone, while only a few of the cartilages in the face are replaced by bone. In fact, the majority of bones comprising the skull form through intramembranous ossification without replacing a cartilaginous template.

A previous report revealed a binary genetic code that determines the fate of each of the skeletal elements (Eames et al., 2004). SOX9 and RUNX2 are transcription factors that regulate the differentiation of chondrocytes (Akiyama et al., 2002; Yan et al., 2002) and osteoblasts (Ducy et al., 1997), and also control the mode of skeletal formation. For instance, *Runx2* is expressed by osteoblasts during intramembranous ossification, and ectopic *Runx2* expression results in differentiation of osteoblasts and intramembranous ossification *in vivo* (Eames et al., 2004). Differentiation of chondrocytes is controlled in part by the action of the transcription factor SOX 9 (Lefebvre et al., 1997; Sekiya et al., 2000; Akiyama et al., 2002). However, whether the cartilage will undergo endochondral

[†]Author for correspondence: Ralph Marcucio, Ph. D., Assistant Professor, UCSF/SFGH, 1001 Potrero Ave, Bldg 9, Room 346, San Francisco, CA, 04110, Ralph.Marcucio@ucsf.edu, Phone: 415-206-5366, Fax: 415-206-8244.

ossification or will remain as persistent cartilage depends on the expression of *Runx2* by chondrocytes. Co-expression of *Runx2* and *Sox9* by chondrocytes leads to replacement of cartilage by bone through endochondral ossification (Eames et al., 2004). In contrast, when *Sox9* expression in chondrocytes is not accompanied by *Runx2*, the cartilage element persists (Eames et al., 2004). The ability of chondrocytes to mature to the hypertrophic stage appears to be related to the presence of an unknown activator protein within the prechondrogenic mesenchyme (Kempf et al., 2007) as well as interactions with the perichondrium (Hinoi et al., 2006). These data suggest that the ability to undergo hypertrophy may be an intrinsic property of each cartilage element and may relate to the competence of chondrocytes to express *Runx2*.

Our objective was to examine the effect of activating or blocking the BMP pathway at various times during development of the facial skeleton, because the majority of these elements do not normally undergo hypertrophy. We examined recruitment of cells to chondrogenic and osteogenic lineages, and we examined the fate of the skeletal elements at late stages of development. Activation of the BMP pathway increased cell proliferation and cartilage size, and our results revealed that mesenchymal cells in the face are plastic and can be directed along chondrogenic pathways even during late developmental periods. Further, the ability of chondrocytes in the mandible to undergo hypertrophy may be controlled by signals from the perichondrium. When these signals are disrupted by Bmps the chondrocytes undergo hypertrophy, but the resulting cartilage elements do not undergo osteogenesis as in the limbs.

Results

Expression of Bmps and receptors in the face

Prior to initiating experimentation to assess the effects of ectopic Bmp signaling on development of the musculoskeletal system of the jaw, we determined the expression patterns of various Bmps and their receptors in the face at various times. At HH 10 *Bmp-2* and *Bmp-4* transcripts were present in the surface ectoderm covering the FNP (Fig. 1A,B). At this time, *Bmp-2* was also expressed within the developing forebrain (Fig. 1A). The receptors, *BmpR1A* and *BmprR1B* were also expressed in the developing head at this time. *BmpR1A* was expressed throughout the mesenchyme, neural ectoderm, and surface ectoderm (Fig. 1C). In contrast, *BmpR1B* expression was more restricted and was found in the forebrain (Fig. 1D). At HH 22 transcripts for *Bmp-2* and *Bmp-4* were observed in the maxillary and mandibular processes. However, their expression patterns were unique. *Bmp-2* was expressed in mesenchymal and ectodermal cells located in medial regions of the maxillary and mandibular processes (Fig. 1E), while *Bmp-4* expression was more prominent in lateral regions of the upper and lower jaw primorida and adjacent ectoderm (Fig. 1F). The Bmp receptors 1A and 1B also exhibited novel expression patterns in these regions. *BmpR1A* was expressed throughout the neural crest mesenchyme in the maxillary and mandibular processes but did not appear to be expressed at high levels in the mesodermal core of the mandible (Fig. 1G). In contrast, *BmpR1B* expression was restricted to the lateral aspects of the mandibular process mesenchyme and was apparent in the mesodermal core of the mandible (Fig. 1H). *BmpR1A* was not expressed in the ectoderm of the maxillary or mandibular process (Fig. 1G), but *BmpR1B* exhibited an interesting expression pattern in these tissues. In the maxillary process, *BmpR1B* was present in the ectoderm located on the ventral surface adjacent to the mandibular process. Likewise, in the mandibular process, this receptor was expressed in ventral ectoderm adjacent to the hyoid process (Fig. 1H).

Blockade of BMP signaling inhibits skeletal formation in the jaw

To determine if BMP signals are required for formation of the skeleton, we performed a loss-of-function experiment by infecting the right mandibular primordium with RCAS encoding the BMP antagonist *Noggin* (RCAS-*Noggin*) at HH 22 and HH 25. When embryos were infected at HH22, we observed truncations of the lower jaw at day 13 (Fig. 2A). Within the lower jaw, we observed that the cartilage and bones on the infected side of the embryo were not present (Fig. 2B,C). When embryos were infected at HH 25 we observed a similar disruption to the skeleton (Fig. 2D–F). In these embryos, we observed some cartilage, but bone formation was inhibited.

BMP signaling stimulates chondrogenesis in the skull

Our next objective focused on assessing the effect of BMP on recruitment of stem cells during development of the head skeleton. We first determined whether the timing of BMP application influenced skeletal development. To achieve our goal we infected the facial mesenchyme with replication competent virus (RCAS) encoding *Bmp-2* or *Bmp-4* at various times of development. We initiated this experiment by infecting mesenchyme of the face at HH11 which is after emigration of the neural crest cells from the neural tube is complete (Tosney, 1982). When embryos this young were infected with RCAS, viral spread was bilateral and a large region of the embryo was infected by the virus. Embryos infected with RCAS-*Bmp-2* or RCAS-*Bmp-4* at this early time point exhibited severe facial malformations at day 9. The upper and lower components of the jaw were short and clefts between the maxillary and frontonasal process were evident (Supplemental Fig. 1). Similarly, embryos analyzed at day 13 exhibited severe facial malformations (Fig. 3A,B; n=15). Analysis of the skeleton at day 13 revealed that a large amount of cartilage had formed in the jaw of these embryos (Fig. 2C–F). The bony skeletal elements in these embryos appeared rudimentary (Fig. 3C,D). Within the frontonasal process the premaxillary and nasal bones were present, but the bones that are derived from the maxillary process appeared as a small nodule within the upper part of the jaw (not shown). In the lower jaw, ossification at the mandibular symphysis was apparent, but the more proximal skeletal elements, the dentary, surangular, and splenial bones, were absent (Fig. 3D). Lastly, in these embryos “strands” of cartilaginous tissues were present in the roof of the skull (Fig. 3E,F). A similar phenotype was observed when embryos were infected (right side only) with the RCAS viruses at HH 15 (Supplemental Fig. 2). Thus, at these early time points, widespread infection with RCAS-*Bmp-2* or *-4* led to up-regulation of BMP signaling throughout the head, which directs the facial mesenchyme to differentiate almost exclusively along chondrogenic pathways.

To assess the effect of ectopic BMP signaling at later time points, we chose to infect the right mandibular prominence using only the RCAS-*Bmp-4* virus. Initially, we focused on embryos infected at HH 22, because this is prior to the overt differentiation of chondrocytes and osteoblasts. Injecting RCAS virions at HH22 led to infection within 24 hours (Fig. 4A). At this time, cartilage was not apparent in infected embryos (Fig. 4E; n=7). Within 48 (n=7) and 72 hours (n=7), the infection had spread (Fig. 4B,C) and noticeable increases in the size of the cartilage anlagen were apparent (Fig. 4F,G). By 96 hours the infection had spread throughout the right side of the mandible (Fig. 4D; n=10), and the cartilage on the infected side was very big (Fig. 4H).

We performed molecular analyses at 96 hours, because at this time Meckel’s cartilage was greatly enlarged (Fig. 4G) and the infection was widespread (Fig. 4C,I,M). In infected embryos the domain of *Col2* expression was expanded (Fig. 4J,N). As expected, this was accompanied by expanded *Sox9* expression (Fig. 4K,O). In contrast, *Runx2* expression appeared to be down regulated (Fig. 4L,P).

These molecular changes resulted in significant alterations in the skeleton at day 14 (n=10). At this time a large cartilaginous mass encompassed the proximal portion of the lower jaw and the hyoid arch (Fig. 6A–F). Furthermore, infection of the mandible at later time points produced similar results. Embryos infected at HH 25 (n=12) and on day 6 (n=12) exhibited increases in the size of Meckel's cartilage at day 13 (Supplemental Fig. 3A,B). When the mandible was infected on day 7 (n=10) only a small increase in the cartilage was observed (Supplemental Fig. 3C), and when embryos were infected on day 8 (n=10), no increase in cartilage was apparent (Supplemental Fig. 3D).

BMP signaling stimulates proliferation, differentiation, and condensation

Our next objective was to determine the mechanism responsible for the formation of the large cartilage mass in the lower jaw. Analysis of sections through the lower jaw at 48 (Fig. 4B; n=7), and 72 (Fig. 4C; n=7) hours after infection indicated that the initial cartilage condensations that formed in treated embryos were larger than normal. When we examined embryos at later times we observed further differentiation of chondrocytes. For example, at day 13 a large cartilage mass was apparent (Fig. 5A), but we also observed new cartilage condensations (Fig. 5B).

In addition to the enhanced differentiation of chondrocytes that we observed, we also determined that at 72 hours after infection cell proliferation was increased (Fig. 5C,D). In control embryos 15% (s.d. 2.2%, n=5) of chondrocytes exhibited incorporation of BrDU, while 29% (s.d. 2.0%, $p<0.0001$, n=5) of chondrocytes in embryos infected with RCAS-*Bmp-4* had incorporated BrDU during the 20 minute chase period. In addition to this increased proliferation in the cartilage anlagen, we observed a dramatic increase in the BrDU-positive mesenchymal cells located adjacent to the cartilage anlagen in all specimens that we examined (Fig. 5C,D, n=5). Collectively, these observations indicate that BMP signaling stimulates proliferation of mesenchymal precursor cells and chondrocytes, induces the earliest phases of chondrocyte differentiation and cartilage condensation.

Cartilages induced by BMPs in the face become hypertrophic

Our final goal was to examine the fate of the cartilages that formed in embryos infected with RCAS-*Bmp-4*. Normally, the cartilage located within the mandible is persistent cartilage and does not become hypertrophic (Fig. 6C,D). Chondrocytes in Meckel's cartilage expressed *Sox9* (Fig. 6G) and *Col2* (Fig. 6H). However, these chondrocytes did not express markers of hypertrophy such as *Col10* (Fig. 6K), *Runx2* (Fig. 6L) or *Ihh* (Fig. 6O; n=10). In the perichondrium, *Runx2* expression (Fig. 6L) was accompanied by expression of *Twist-1* (Fig. 6P) and *Fgf18* (Fig. 6T), and in the limb bud, these molecules work in series to suppress hypertrophy in chondrocytes (Hinoi et al., 2006). After infection with RCAS-*Bmp-4* (n=7) some of the chondrocytes in the cartilage mass of the jaw exhibited signs of hypertrophy (Fig. 6E,F) and expressed *Sox9* (Fig. 6I), *Col2* (Fig. 6J), *Col10* (Fig. 6M), *Runx2* (Fig. 6N), *Ihh* (Fig. 6Q), and *Noggin* (Fig. 6U). Furthermore, in large regions of the cartilages in infected embryos there was no evidence of a perichondrium (Fig. 7B), and expression of *Runx2* (Fig. 6N), *Twist-1* (Fig. 6R), and *Fgf18* (Fig. 6V) was either down-regulated or absent. Thus, by day 14, chondrocyte hypertrophy was evident in cartilage located within the lower jaw of treated embryos and changes in the perichondrium or blockade of Bmp signaling within the cartilage may have been responsible for these changes.

In the appendicular skeleton, once chondrocytes become hypertrophic, vascular invasion of the cartilage matrix occurs, and bone forms behind this wave of invading vasculature (Colnot and Helms, 2001). This process of endochondral ossification results in the replacement of the cartilage template by bone. Since we observed hypertrophic chondrocytes in the jaw we naturally thought that this cartilage would be replaced by bone.

Therefore, we examined the cartilages prior to hatching at day 19 (Fig. 7A–D; n=6). We observed a large amount of cartilage (Fig. 7A) comprised of hypertrophic chondrocytes (Fig. 7B,C) in these embryos. At this time chondrocytes were still expressing high levels of *Col10* (Supplemental Fig. 4) and *Runx2* (not shown), while *Sox9* and *Col2* transcripts were detectable but appeared down-regulated at this time (Supplmental Fig. 4). Although we did not observe replacement of the cartilage by bone at this time, we did observe evidence of vascular invasion of the cartilage matrix (Fig. 7C,D).

To make sure that enough time had passed for us to observe endochondral ossification after chondrocyte hypertrophy had begun, we transplanted infected cartilage condensations from day 11 embryos under the renal capsule of immuno-compromised mice. When the cartilage anlagen of murine long bones were transplanted into the renal capsule, the normal process of endochondral ossification was observed (Colnot et al., 2004; Colnot et al., 2005). First, we placed Meckel's cartilage from an uninfected embryo (n=2) under the renal capsule of immuno-deficient mice for 4 weeks. We observed no changes in the cartilage that resembled endochondral ossification or vascular invasion (Fig. 7E,F). Further, when we repeated this experiment with Meckel's cartilage that had been infected with RCAS-*Bmp4*, we observed no evidence of endochondral ossification at 2 (n=2, not shown), 3 (n=2, not shown) and 4 weeks (Fig. 7G; n=4) even though the chondrocytes were hypertrophic at these times. As at day 19 *in ovo* we observed vascular invasion of the infected cartilage (Fig. 7H). Thus, sustained BMP signaling stimulates chondrocyte differentiation and hypertrophy in cranial mesenchyme, but the cartilage fails to undergo endochondral ossification.

Effect of ectopic BMP signaling on bone formation

When embryos were infected at HH22, the increase in cartilage formation was obvious by gross examination of the skeletal preparations and histological sections. However, the effects of BMPs on osteogenesis were less clear even though *Runx2* expression appeared to be down-regulated at 96 hours after infection (Fig. 4L,P). Therefore, a histomorphometric analysis of the bone in treated embryos was performed to determine how BMP signaling affected osteogenesis. The volume of bone that formed in the lower jaw of embryos infected with RCAS-Bmp-4 (0.55 mm^3 s.d.=0.25; n=5) was less than in control embryos (0.88 mm^3 s.d.=0.19; n=4), but this only approached statistical significance (p=0.06). However, we observed other alterations in the bones that suggested BMP signaling negatively affected osteogenesis. For example, when embryos were infected at HH11, the roof of the skull became cartilaginous rather than bony (Fig. 3F). Further, in embryos that were infected at HH22, HH25, day 6, day 7, and day 8 (total n=30) we observed that in each case the periosteum was severely disrupted (Fig. 8B). Normally, the periosteum forms two very well-defined layers of cells adjacent to the bone (Fig. 8A). However, in embryos infected with RCAS-*Bmp-4* there was no evidence of a defined periosteum. Instead mesenchymal cells surrounded the bone (Fig. 8B).

Discussion

Bone morphogenetic proteins are potent skeletogenic molecules. In this work, we first determined that Bmp signaling is required for skeletogenesis in the jaw. Next we demonstrated that activation of the BMP pathway expanded the expression domain of *Sox9* and increased the amount of cartilage that formed. This result is not surprising given that ectopic expression of *Sox9* increases cartilage formation in the pharyngeal arches (Eames et al., 2004). Further, our data agrees with a previous report indicating that infection with these viruses of neural crest cells that will give rise to the frontal bone induces chondrogenesis (Abzhanov et al., 2007). Then we determined that the increased cartilage resulted from increased proliferation of precursor cells in the mesenchyme and stimulation of chondrocyte differentiation and proliferation. Interestingly, we observed evidence of chondrocyte

hypertrophy in infected embryos even though these elements normally persistent as cartilage. However, we were surprised that these cartilage elements did not undergo endochondral ossification and subsequent replacement by bone. In contrast to these anabolic effects on cartilage, ectopic BMP signaling did not stimulate intramembranous ossification. Rather intramembranous ossification appeared to be suppressed. This observation is somewhat surprising since BMP signaling is required for bone formation (e.g., (Chen et al., 1997) and reviewed in (Cao and Chen, 2005) and see Fig. 7), but this observation agrees with recent data that illustrates a similar effect of BMP signaling on development of the frontal bone (Abzhanov et al., 2007). Collectively, our data reveal that by altering the levels of Bmp signaling within the developing jaw, the skeletal system can be altered. This system will provide us with a method to elucidate mechanisms that regulate the ability of cartilage to be maintained in a prehypertrophic state, and this could have significant clinical application. For instance, inhibition of chondrocyte hypertrophy could be applied to tissue engineering approaches aimed at resurfacing articular surfaces.

BMP signaling promotes chondrogenesis in cranial mesenchyme

The differences in skeletogenesis that occurs in the face and limbs suggest that regulation of skeletal formation in these regions may be unique and have led others to investigate formation of the facial skeleton in this light (e.g., (Barlow and Francis-West, 1997; Ashique et al., 2002; Mina et al., 2002)). BMP signaling participates in regulating development of the skeleton of the face. Transient upregulation of BMP signaling through application of BMP-soaked beads to the maxillary and mandibular process of avian embryos alters the size of the skeletal elements that form in the jaw possibly by altering proliferation and death of skeletal progenitor cells (Barlow and Francis-West, 1997). Previous work has illustrated that BMP signaling does not participate in growth of the mandibular primordium, but this work (Mina et al., 2002), and our work, indicates that BMP signaling stimulates chondrocyte differentiation in the mandible. The pro-chondrogenic potential of BMP signaling in birds is likely to be mediated by Bmp receptor Type 1b (Ashique et al., 2002), and this receptor is expressed by the skeletal precursors in the mandibular process at HH22.

The timing and levels of BMP signaling appear to regulate chondrogenesis and osteogenesis. In the limb a cartilage template forms first, and then is subsequently replaced by bone. Both of these processes are regulated by Bmp signaling (reviewed in: (Cao and Chen, 2005)). However, in the head development of bone and cartilage occurs virtually simultaneously. Furthermore, the cells that comprise the bone and cartilage arise from a common population of precursor cells. Our data clearly demonstrate that both tissue types require BMP signaling for formation. For example, blockade of BMP signaling during early stages of skeletogenesis hinders formation of both bone and cartilage. In contrast, when we blocked BMP signaling at slightly later stages bone was more severely affected than cartilage. Yet, activation of the BMP pathway increased chondrogenesis at the expense of bone. These data illustrate that the levels and timing of BMP signaling during formation of cartilage and bone must be tightly regulated to ensure adequate differentiation of both of these tissue types. How Bmps act to regulate these processes, especially when the ligands are expressed broadly, is paradoxical but may involve modulation by extracellular antagonists and intracellular cofactors (Reviewed in: (Rosen, 2006)).

The mode of skeletal development can be altered by BMP signaling

In addition to the role of Bmps in regulating commitment to skeletal lineages, we were also interested in examining the effect of exogenous BMP signaling on the mode of skeletal formation. Previous work has indicated that BMPs stimulate heterotopic bone formation through both intramembranous and endochondral ossification in adult animals (reviewed in: (Wozney and Rosen, 1998)). However, in the developing limb bud, ectopic BMP signaling

increased production of cartilage and almost completely suppressed formation of bone (Duprez et al., 1996b). The absence of bone in these embryos was explained by a delay of chondrocyte hypertrophy, and failure of endochondral ossification in these embryos. In our work, ectopic cartilages that formed within the jaw exhibited morphological and molecular signs of hypertrophy and exhibited signs of limited vascular invasion, but did not undergo endochondral ossification. The chondrocytes expressed *Col10* which is a marker of chondrocyte hypertrophy. Additionally, these cells expressed the transcription factor *Runx2* which regulates chondrocyte hypertrophy (Reviewed in: (Solomon et al., 2008)). Furthermore, chondrocytes in these condensations expressed the signaling molecule *Ihh*. This observations is not surprising since BMP signaling has been shown to directly regulate *Ihh* expression (Seki and Hata, 2004). During development of the long bones IHH regulates proliferation and hypertrophy of chondrocytes and differentiation of osteoblasts in the adjacent perichondrium (Vortkamp et al., 1996; St-Jacques et al., 1999; Chung et al., 2001). Therefore, we presume that the increased proliferation and hypertrophy of chondrocytes that we observed was linked to Ihh up-regulation. However, in the absence of a functional perichondrium, subsequent endochondral ossification did not occur.

Interestingly, continual interaction between the perichondrium and chondrocytes regulates proliferation and hypertrophy in the limb bud. *Runx2* that is expressed in the perichondrium inhibits hypertrophy in adjacent chondrocytes through the action *Fgf18* (Hinoi et al., 2006). We determined that these molecules are normally expressed in the perichondrium that surrounds Meckel's cartilage suggesting that they may suppress hypertrophy throughout this element. In our gain-of-function experiments we observed a loss of *Runx2* and *Fgf18* throughout large regions of the perichondrial region in infected embryos. These changes could have directly contributed to the hypertrophy that we observed by relieving a repressive influence on the chondrocytes. Additionally, we observed up-regulation of the Bmp antagonist *Noggin* in the chondrocytes. Blockade of Bmp signaling could have also contributed to the hypertrophy in these cartilages.

In light of the changes in the cartilages after activation of the BMP pathway, one would have predicted that these elements would have been replaced by bone. However, these cartilages did not show signs of endochondral ossification. The reason for this paradox is unknown, but these cartilage elements did not have a well-developed perichondrium. The perichondrium is a source of osteoblasts that form bone during endochondral ossification (Colnot et al., 2004). Therefore, we speculate that the cartilage matured and was capable of inducing vascular invasion, but the absence of osteoblast precursors in the perichondrium precluded replacement by bone. Thus, Bmp signaling during development of the normal jaw skeleton must be distinct from that in the limb. However, the basis for this distinction is not known.

In summary, our results reveal that exogenous BMP signaling stimulates chondrogenesis, but not sufficient for osteogenesis. Our work suggests that a primary role of BMP signaling could be to regulate cell differentiation within the developing musculoskeletal system of the face. High or sustained levels of BMP signaling converts osteogenic cells to the chondrogenic lineage and transforms persistent cartilages into replacement cartilages. Thus, highly co-ordinated signaling by the BMP pathway generates the tissues within the skeleton of the head.

Experimental Procedures

Production of RCAS-Bmp-2, RCAS-Bmp-4, RCAS-Noggin, and RCAS-AP

Replication competent retroviruses (RCAS) encoding *Bmp-2* (Duprez et al., 1996a), *Bmp-4* (Duprez et al., 1996a), *Noggin* (Capdevila and Johnson, 1998) or Alkaline Phosphatase

(Fekete and Cepko, 1993) have been previously described and were produced by standard methods (Morgan and Fekete, 1996). DF-1 (ATCC, Manassus, VA) cells were grown to 70% confluence and then were transfected (Transfection Reagent, Qiagen) with plasmids to produce each virus. Viral supernatants were collected by ultracentrifugation and stored at −80C until use. All viral titers were $>10^9$.

Preparation of embryos and infection of embryos with RCAS viruses

Fertilized chicken eggs (*Gallus gallus*, Charles River, SPAFAS) were prepared for surgical manipulations as follows. Embryos were incubated to Hamburger and Hamilton stage 10 (HH 10 (Hamburger and Hamilton, 1951) (approximately 36 hours)) and then a small hole was made in the shell directly over the embryo after removing 1.0ml of albumin. The hole was covered with tape and the embryos were returned to the incubator. Once embryos reached HH 11, HH 22, HH 25, day 5, day 6, day 7, or day 8 of development the tape was removed and the mandibular process was injected with viral particles (0.l to 0.15μl).

Histology and histomorphometry

Embryos, collected at various times (24, 48, 72, and 96 hours after infection, and 8, 9, 10, 13, 14, 15, 17, and 19 days of development) were fixed in 4% paraformaldehyde, photographed, dehydrated, embedded in paraffin, and sectioned (10μm). Alternatively, older embryos were processed for cartilage and bone staining with Alcian blue and alizarin red (Wassersug, 1976). Sections were stained with Safranin-O/Fast Green to visualize cartilage, modified Milligan's Trichrome to visualize bone. The proportion of bone in treated and control mandibles infected at HH 22 was determined on day 14 using Photoshop to estimate the number of pixels comprising bone in every fifteenth section. The number of pixels comprising bone was converted to an estimate of the area of bone, and then the volume of the bone (VB) in mandibles was calculated using the following equation: $VB=1/3*h*(A_1+A_2*\sqrt{A1*A2})$. A_1 and A_2 are the area of the bone in the sequential sections that were measured, and h is the distance between A_1 and A_2 (Colnot et al., 2003; Lu et al., 2005). A paired t-test was used to determine whether Bmp treatment affected formation of bone matrix.

In situ hybridization

Patterns of gene expression were analyzed by *in situ* hybridization using radiolabeled riboprobes as previously described (Albrecht et al., 1997). Subclones of *Bmp-2*, *Bmp-4*, *Bmp-R1a*, *Bmp-R1b*, *vENV*, *Sox9*, *Runx2*, *Ihh*, *Twist-1*, *Fgf18*, *Col2*, and *Col10* were linearized to transcribe ^{35}S-labeled riboprobes. Images of *in situ* hybridization assays are Photoshop pseudo-colored superimpositions of the *in situ* hybridization signal and a blue nuclear stain (Hoechst Stain; Sigma).

Cell proliferation—At 72 hours after infection 200nl of BrdU labeling reagent (Zymed, South San Francisco, CA) was injected into the vitellein vein. Embryos were returned to the incubator for 20 minutes, then were fixed, embedded, and sectioned. BrdU labeled cells were visualized on paraffin sections; detection of BrdU incorporation was assessed by immunohistochemistry and detection with diaminobenzidine (DAB) followed by counterstaining all nuclei with hematoxylin following the manufacturer's instructions (Zymed). The proportion of BrDU-positive cells in the cartilage was determined by uniform, random sampling using the Olympus CAST. Students t-test was used to assess significance.

Renal capsule transplant

Skeletal elements were collected at 11 of development. Each skeletal element was separated in three portions that were transplanted underneath the renal capsule of Nude mice following

a protocol previously described in (Colnot et al., 2004). Control skeletal elements were cut in two portions before transplantation. Cartilage hypertrophy, vascular invasion and bone formation were assessed by histology 2 weeks, 3 weeks and 4 weeks post-transplant. All work was approved by the UCSF IACUC.

Supplementary Material

Refer to Web version on PubMed Central for supplementary material.

Acknowledgments

We would like to thank Drs Richard Schneider, Amy Merrill, Chuanyong Lu, and Brian Eames for helpful discussions throughout the course of this project. This work was funded by the UCSF Research Evaluation and Allocation Committee and the National Institutes of Health, (NIDCR (R03-DE015901 and R01-1DE018234)) to R.M..

Grant information: NIDCR R03-DE015901, R01-1DE018234-01, and UCSF Research Evaluation and Allocation Committee to R.M.

References

Abzhanov A, Rodda SJ, McMahon AP, Tabin CJ. Regulation of skeletogenic differentiation in cranial dermal bone. Development. 2007; 134:3133–3144. [PubMed: 17670790]

Akiyama H, Chaboissier MC, Martin JF, Schedl A, de Crombrugghe B. The transcription factor Sox9 has essential roles in successive steps of the chondrocyte differentiation pathway and is required for expression of Sox5 and Sox6. Genes Dev. 2002; 16:2813–2828. [PubMed: 12414734]

Albrecht, UEG.; Helms, JA.; Lin, H. Visualization of gene expression patterns by in situ hybridization. In: Daston, GP., editor. Molecular and cellular methods in developmental toxicology. Boca Raton, FL: CRC Press; 1997. p. 23-48.

Ashique AM, Fu K, Richman JM. Signalling via type IA and type IB bone morphogenetic protein receptors (BMPR) regulates intramembranous bone formation, chondrogenesis and feather formation in the chicken embryo. Int J Dev Biol. 2002; 46:243–253. [PubMed: 11934153]

Barlow AJ, Francis-West PH. Ectopic application of recombinant BMP-2 and BMP-4 can change patterning of developing chick facial primordia. Development. 1997; 124:391–398. [PubMed: 9053315]

Cao X, Chen D. The BMP signaling and in vivo bone formation. Gene. 2005; 357:1–8. [PubMed: 16125875]

Capdevila J, Johnson RL. Endogenous and ectopic expression of noggin suggests a conserved mechanism for regulation of BMP function during limb and somite patterning. Dev Biol. 1998; 197:205–217. [PubMed: 9630747]

Chen D, Harris MA, Rossini G, Dunstan CR, Dallas SL, Feng JQ, Mundy GR, Harris SE. Bone morphogenetic protein 2 (BMP-2) enhances BMP-3, BMP-4, and bone cell differentiation marker gene expression during the induction of mineralized bone matrix formation in cultures of fetal rat calvarial osteoblasts. Calcif Tissue Int. 1997; 60:283–290. [PubMed: 9069167]

Chung, U-i; Schipani, E.; McMahon, AP.; Kronenberg, HM. Indian hedgehog couples chondrogenesis to osteogenesis in endochondral bone development. Journal of Clinical Investigation. 2001; 107:295–304. [PubMed: 11160153]

Colnot C, de la Fuente L, Huang S, Hu D, Lu C, St-Jacques B, Helms JA. Indian hedgehog synchronizes skeletal angiogenesis and perichondrial maturation with cartilage development. Development. 2005; 132:1057–1067. [PubMed: 15689378]

Colnot C, Lu C, Hu D, Helms JA. Distinguishing the contributions of the perichondrium, cartilage, and vascular endothelium to skeletal development. Dev Biol. 2004; 269:55–69. [PubMed: 15081357]

Colnot C, Thompson Z, Miclau T, Werb Z, Helms JA. Altered fracture repair in the absence of MMP9. Development. 2003; 130:4123–4133. [PubMed: 12874132]

Colnot CI, Helms JA. A molecular analysis of matrix remodeling and angiogenesis during long bone development. Mech Dev. 2001; 100:245–250. [PubMed: 11165481]

Ducy P, Zhang R, Geoffroy V, Ridall AL, Karsenty G. Osf2/Cbfa1: a transcriptional activator of osteoblast differentiation. Cell. 1997; 89:747–754. [PubMed: 9182762]

Duprez D, Bell EJ, Richardson MK, Archer CW, Wolpert L, Brickell PM, Francis-West PH. Overexpression of BMP-2 and BMP-4 alters the size and shape of developing skeletal elements in the chick limb. Mech Dev. 1996a; 57:145–157. [PubMed: 8843392]

Duprez D, Bell EJ, Richardson MK, Archer CW, Wolpert L, Brickell PM, Francis-West PH. Overexpression of BMP-2 and BMP-4 alters the size and shape of developing skeletal elements in the chick limb. Mechanisms of Development. 1996b; 57:145–157. [PubMed: 8843392]

Eames BF, Sharpe PT, Helms JA. Hierarchy revealed in the specification of three skeletal fates by Sox9 and Runx2. Developmental Biology. 2004; 274:188–200. [PubMed: 15355797]

Fekete DM, Cepko CL. Replication-competent retroviral vectors encoding alkaline phosphatase reveal spatial restriction of viral gene expression/transduction in the chick embryo. Mol Cell Biol. 1993; 13:2604–2613. [PubMed: 8455633]

Hamburger V, Hamilton HL. A series of normal stages in the development of the chick embryo. Journal of Morphology. 1951; 88:49–92.

Hinoi E, Bialek P, Chen YT, Rached MT, Groner Y, Behringer RR, Ornitz DM, Karsenty G. Runx2 inhibits chondrocyte proliferation and hypertrophy through its expression in the perichondrium. Genes Dev. 2006; 20:2937–2942. [PubMed: 17050674]

Kempf H, Ionescu A, Udager AM, Lassar AB. Prochondrogenic signals induce a competence for Runx2 to activate hypertrophic chondrocyte gene expression. Dev Dyn. 2007; 236:1954–1962. [PubMed: 17576141]

Lefebvre V, Huang W, Harley VR, Goodfellow PN, de Crombrugghe B. SOX9 is a potent activator of the chondrocyte-specific enhancer of the pro alpha1(II) collagen gene. Mol Cell Biol. 1997; 17:2336–2346. [PubMed: 9121483]

Lu C, Miclau T, Hu D, Hansen E, Tsui K, Puttlitz C, Marcucio RS. Cellular basis for age-related changes in fracture repair. J Orthop Res. 2005; 23:1300–1307. [PubMed: 15936915]

Mina M, Wang YH, Ivanisevic AM, Upholt WB, Rodgers B. Region- and stage-specific effects of FGFs and BMPs in chick mandibular morphogenesis. Dev Dyn. 2002; 223:333–352. [PubMed: 11891984]

Morgan, BA.; Fekete, DM. Manipulating gene expression with replication-competent retroviruses. Academic Press; 1996.

Rosen V. BMP and BMP inhibitors in bone. Ann N Y Acad Sci. 2006; 1068:19–25. [PubMed: 16831902]

Seki K, Hata A. Indian hedgehog gene is a target of the bone morphogenetic protein signaling pathway. J Biol Chem. 2004; 279:18544–18549. [PubMed: 14981086]

Sekiya I, Tsuji K, Koopman P, Watanabe H, Yamada Y, Shinomiya K, Nifuji A, Noda M. SOX9 enhances aggrecan gene promoter/enhancer activity and is up-regulated by retinoic acid in a cartilage-derived cell line, TC6. J Biol Chem. 2000; 275:10738–10744. [PubMed: 10753864]

Solomon LA, Berube NG, Beier F. Transcriptional regulators of chondrocyte hypertrophy. Birth Defects Res C Embryo Today. 2008; 84:123–130. [PubMed: 18546336]

St-Jacques B, Hammerschmidt M, McMahon AP. Indian hedgehog signaling regulates proliferation and differentiation of chondrocytes and is essential for bone formation. Genes and Development. 1999; 13:2072–2086. [PubMed: 10465785]

Tosney KW. The segregation and early migration of cranial neural crest cells in the avian embryo. Developmental Biology. 1982; 89:13–24. [PubMed: 7054004]

Vortkamp A, Lee K, Lanske B, Segre GV, Kronenberg HM, Tabin CJ. Regulation of rate of cartilage differentiation by Indian hedgehog and PTH-related protein. Science. 1996; 273:613–622. [PubMed: 8662546]

Wassersug R. A procedure for differential staining of cartilage and bone in whole formalin-fixed vertebrates. Stain Technology. 1976; 51:131–134. [PubMed: 59420]

Wozney JM, Rosen V. Bone morphogenetic protein and bone morphogenetic protein gene family in bone formation and repair. Clin Orthop Relat Res. 1998:26–37. [PubMed: 9577407]

Yan YL, Miller CT, Nissen RM, Singer A, Liu D, Kirn A, Draper B, Willoughby J, Morcos PA, Amsterdam A, Chung BC, Westerfield M, Haffter P, Hopkins N, Kimmel C, Postlethwait JH, Nissen R. A zebrafish sox9 gene required for cartilage morphogenesis. Development. 2002; 129:5065–5079. [PubMed: 12397114]

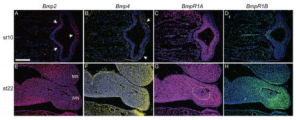

Figure 1. Bone morphogenetic proteins and receptors are expressed in the mandibular and maxillary process of avian embryos prior to skeletogenesis

(**A**) *Bmp-2* (red) was expressed in the forebrain (arrows) and surface ectoderm at HH 10, but (**B**) *Bmp-4* (yellow) expression was restricted to the ectoderm (arrows). Sections were counterstained with bis-benzimide. (**C**) *BmpR1A* transcripts (pink) were detected throughout the mesenchyme and the epithelia of the head at this time. (**D**) In contrast, *BmpR1B* (green) was expressed only in the forebrain. (**E**) At HH 22, *Bmp-2* transcripts (red) were detected in the mesenchyme and the epithelia of the maxillary (Mx) and mandibular (Mn) processes. (**F**) Similarly, *Bmp-4* (yellow) was expressed in mesenchyme and epithelia of facial primorida. These transcripts were more abundant in lateral regions of the upper and lower jaw primordial. (**G**) *Bmp-R1A* (pink) was detected throughout the mesenchyme of the maxillary and mandibular processes, but was excluded from the middle of the mesodermal core (dotted circle). (**H**) *Bmp-R1B* (green) was restricted to lateral regions of the lower jaw including the mesoderm (circled), and was less widespread in the maxillary process compared to Bmp-Receptor 1A. Scale bars: 200μm.

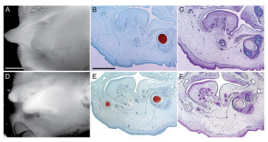

Figure 2. BMP signaling is required for chondrogenesis and osteogenesis

(**A**) Ventral view of the lower jaw of an embryo infected with RCAS-*Noggin* at HH22 and allowed to develop to day 13. The lower jaw was foreshortened. (**B**) SafraninO and (**C**) modified Milligan's trichrome staining demonstrates that blocking BMP signaling abrogated development of the cartilage and bone. (**D**) When embryos were infected with RCAS-*Noggin* at HH25 we observed a similar phenotype. The lower jaw was smaller. (**E**) SafraninO staining demonstrates that Meckel's cartilage was smaller in the infected jaw (left side of photo), and (**F**) modified Milligan's trichrome stain demonstrated the absence of bone in the lower jaw. Scale bars: A,D: 250μm, B,C,E,F: 100μm.

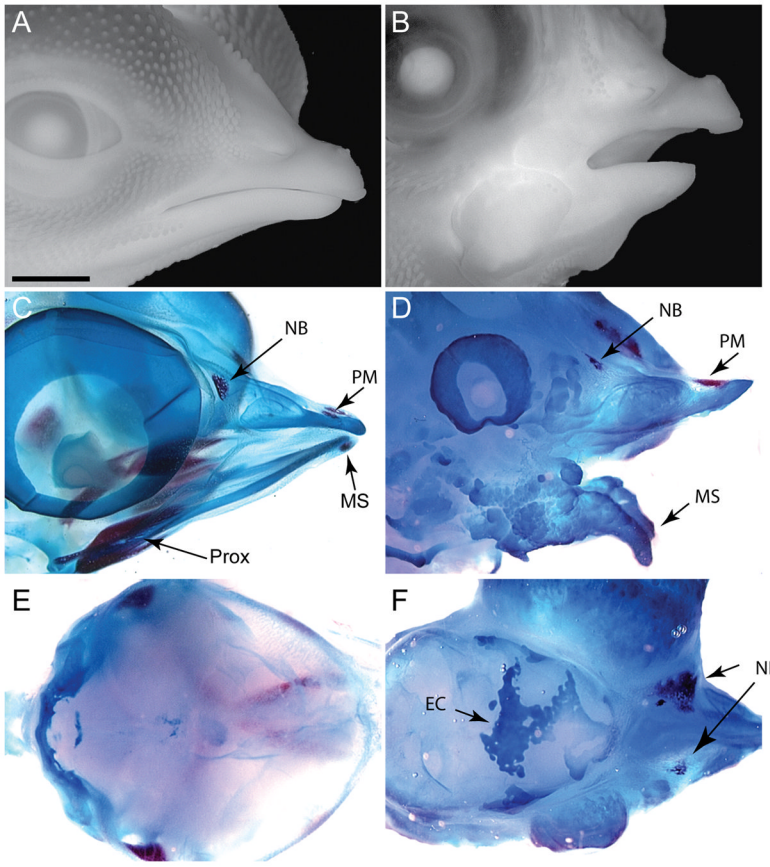

Figure 3. Embryos infected with RCAS-Bmp at HH11 produce large amounts of cartilage at the expense of bone

(**A**) Side view of a normal embryo at day 13. (**B**) Embryos infected with RCAS-*Bmp-2* or RCAS-*Bmp-4* exhibit severe malformations. In this embryo, the lower jaw was truncated and dysmorphic. (**C**) Whole skeletal preparations stained with alcian blue (cartilage) and alizarin red (bone) reveal that normally at this time the nasal bone (NB), the premaxillary bone (PM), and bones in the proximal jaw (Prox) and the mandibular symphsis (MS) are evident. The cartilage elements of the upper and lower jaw are also in place. (**D**) In embryos infected with RCAS-*Bmp-2* or *Bmp-4* a large amorphous cartilaginous mass is apparent in the upper and lower jaw. The nasal bone (NB), premaxillary bone (pM) and the mandibular symphysis are rudimentary. (**E**) Dorsal view of the roof of the skull demonstrating that normally, the bones have not formed by this time. (**F**) Embryos infected with RCAS-*Bmp-2* or *Bmp-4* have ectopic cartilage (EC) covering the brain Scale bar: 250μm.

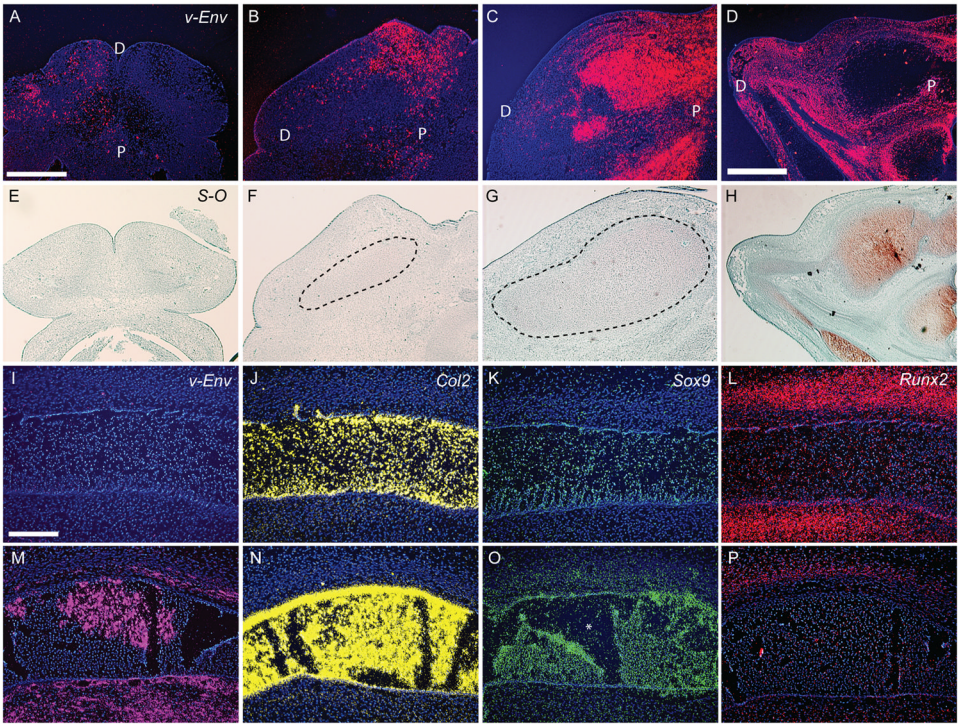

Figure 4. Ontogeny of changes in infected embryos

(**A**) At 24 hours after infection transcripts for the viral envelope gene (vENV; red) were present in small regions of the lower jaw. (**B**) By 48, (**C**) 72, and (**D**) 96 hours after injection of RCAS-Bmp-4, the infection spread progressively. (**E**) Safranin-O staining of infected embryos at 24 hours reveals no evidence of cartilage formation. (**F**) However, within 48 hours the cartilage forming in treated embryos was expanded. (**G**) By 72 and (**H**) 96 hours the cartilage in treated embryos was grossly oversized. (**I**) Normal embryos (n=6) were not infected with RCAS. (**J**) *Col2* transcripts (yellow) were present in Meckel's cartilage at the time of analysis (72 hours post-infection). (**K**) *Sox-9* expression (green) was restricted to Meckel's cartilage at this time. (**L**) *Runx2* (red) was expressed in domains adjacent to Meckel's cartilage. (**M**) Infected embryos (n=10) exhibit widespread expression of the viral envelope gene (pink). (**N**) In treated embryos, *Col2* transcripts were restricted to Meckel's cartilage, but (**O**) *Sox-9* transcripts were detected in the cartilage and the adjacent mesenchyme. P=proximal, D=distal, * denotes a tear in the cartilage. (**P**) Expression of *Runx2* appears down-regulated. Scale bars: 200μm.

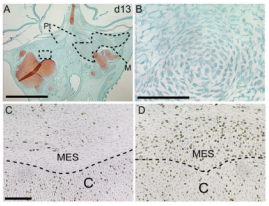

Figure 5. Proliferation and condensation are enhanced in treated embryos

(**A**) At day 13, a large cartilage mass is evident in treated embryos. Further, jaw muscles are apparent on the non-infected side (dotted line), and are not present on the infected side. (**B**) Higher magnification of boxed area in A illustrates the presence of a cellular condensation. This condensation is just faintly stained with safraninO indicating this is a newly formed cartilage mass. (**C**) Control embryo illustrating BrDU incorporation in chondrocytes (C) and mesenchymal cells (MES). (**D**) After treatment with RCAS-Bmp-4 incorporation of BrDU in the mesenchyme is greatly enhanced. M=muscle, Pt=ptyergoid bone. scale bars A: 250μm, B-D: 100μm.

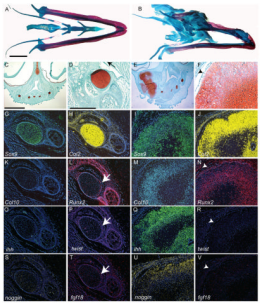

Figure 6. Morphological and molecular alterations of the jaw

(A) Alcian Blue and Alizarin Red staining illustrates the cartilage (blue) and bone (red) elements comprising the tongue and mandible of chick embryos incubated for 15 days (n=3). (**B**) In treated embryos (HH22) incubated for 14 days (n=10), the jaw and tongue skeleton exhibit increased cartilage formation. (**C**) A transverse section, stained with safranin-o and fast green, through the tongue and lower jaw of an embryo incubated for 14 days illustrates the normal morphology of the cartilages (red) that comprise the skeleton. (**D**) Higher magnification of Meckel's cartilage (red) of the lower jaw. (**E**) A section through a treated embryo reveals the large amount of cartilage that formed in response to BMP signaling. (**F**) Higher magnification of cartilage in E shows chondrocytes that appear to be hypertrophic. These cartilages do not have a well-formed perichondrium (arrowhead). (**G**) *Sox9* (green) expression was normally restricted to the developing cartilages, where (**H**) *Col2* (yellow) was also expressed. *Col2* transcripts were also detected in mesenchymal cells adjacent to the cartilage. (**I**) In treated embryos the *Sox9* and (**J**) *Col2* expression domains were expanded, but their spatial patterns are not altered. (**K**) Normally, *Col10* was not expressed by Meckel's cartilage, and (**L**) *Runx2* was only expressed in the adjacent bones and the perichondrium (arrow). (**M**) However, in the hypertrophic chondrocytes located in the ectopic cartilages, *Col10* and (**N**) *Runx2* transcripts were present. In the perichondrium (arrowhead), *Runx2* transcripts were down-regulated in some regions, and not detected in others (not shown). (**O**) *Ihh* was not normally expressed in Meckel's cartilage. (**P**) *Twist-1* (purple) transcripts were detected in the perichondrium of normal Meckel's cartilage. (**Q**) *Ihh* transcripts were detected in chondrocytes of treated cartilage. (**R**) *Twist-1* was not detected in the perichondrium of treated embryos. (**S**) Normally, *Noggin* was not expressed by mandibular chondrocytes. (**T**) *Fgf18* transcripts (pink) were detected in the perichondrium of Meckel's cartilage. (**U**) After infection with RCAS-*Bmp-4 Noggin* expression was upregulated in chondrocytes. (**V**) *Fgf18* transcripts were absent from the perichondrial region of treated cartilage. A,B,C,E: 250μm, D,F,G-V: 200μm

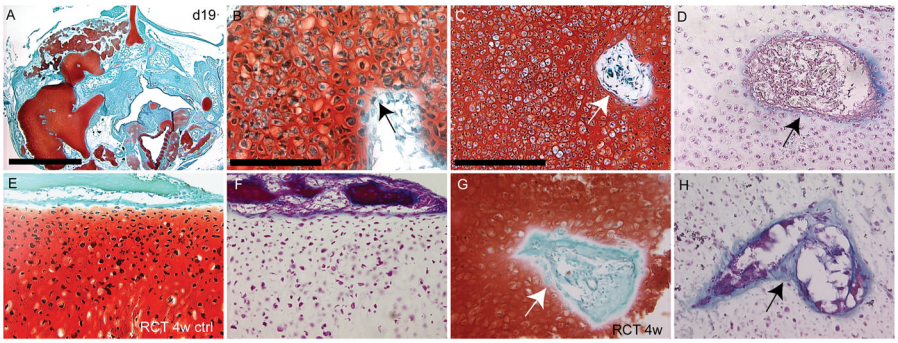

Figure 7. Fate of ectopic cartilage

(**A**) At day 19, many cartilage nodules were present in the infected side of the embryos. (**B**) Some of these chondrocytes appeared hypertrophic, and there was no evidence of a perichondrial layer (arrow) around these cartilages. (**C**) Blood vessel invasion was evident in the cartilage after safranin-O and (**D**) Trichrome staining (arrows). (**E**) Safranin-O staining of normal cartilage that had been under the renal capsule for 4 demonstrated that there were no hypertrophic chondrocytes present. (**F**) Trichrome staining of an adjacent section revealed that there endochondral ossification was not occurring. (**G**) Safranin-O staining of infected cartilage revealed many hypertrophic chondrocytes, and invasion by blood vessels (arrow). (**H**) Staining with modified Milligan's trichrome indicated that the cartilage was not being replaced by bone, but was invaded by vasculature (arrow). scale bars A: 250μm, B: 100μm, C-H: 200μm.

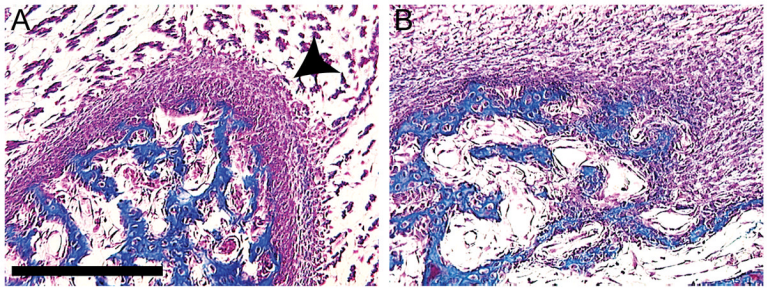

Figure 8. Malformations of bone in treated embryos

(**A**) Normally at day 13, a thickened periosteal layer (arrowhead) is present on the outside of developing bone. (**B**) However, an embryo infected with RCAS-*Bmp-4* at HH22 demonstrates that the periosteum is absent from bones. Scale bar: 200μm.